

In-Reactor Polypropylene Functionalization – The Influence of Catalyst Structure and Reaction Conditions on Catalytic Performance

Miloud Bouyahyi,^{*a} Lidia Jasinska-Walc,^b Rob Duchateau^{*a,c}

Muhammad Naseem Akhtar,^{*d} E. A. Jaseer,^d Rajesh Theravalappil^d Nestor Garcia^d

^a SABIC Technology & Innovation, STC Geleen, Urmonderbaan 22, Geleen, the Netherlands.

^b Department of Polymer Technology, Chemical Faculty, Gdansk University of Technology, G. Narutowicza Str. 11/12, 80-233 Gdansk, Poland.

^c Engineering and Technology Institute Groningen, University of Groningen, Nijenborgh 4, 9747 AG Groningen, The Netherlands.

^d Center for Refining and Advanced Chemicals, Research Institute, King Fahd University of Petroleum & Minerals, Dhahran, Saudi Arabia.

ABSTRACT

To unravel the relationship between silylene-bridged metallocene catalyst structures and polymerization conditions on the performance in in-reactor functionalization of polypropylene, the behavior of *rac*-Me₂Si(2-Me-4-Ph-Ind)₂ZrCl₂/MMAO, *rac*-Me₂Si(Ind)₂ZrCl₂, *rac*-Me₂Si(2-Me-4-Ph-Ind)₂HfCl₂ and *rac*-Me₂Si(Ind)₂HfCl₂ in propylene/aluminum alkyl-passivated 10-undecen-1-ol copolymerization was compared. Kinetic analysis revealed higher catalytic activities for zirconocenes compared to analogous hafnocenes. Both the zirconocene and hafnocene with substituted indenyl ligands afforded higher molecular weight capability, improved stereo-selectivity and enhanced ability to incorporate functionalized comonomer compared to their non-substituted congeners. An in-depth study of polypropylene functionalization using the best performing catalyst system, *rac*-Me₂Si(2-Me-4-Ph-Ind)₂ZrCl₂/MMAO, at temperatures ranging from 40 to 100 °C revealed a linear inversely proportional correlation of polymerization temperature with functionalized comonomer reactivity ($\nearrow T_p \rightarrow \searrow r_1$), copolymer molecular weight ($\nearrow T_p \rightarrow \searrow M_n$), and melting temperature ($\nearrow T_p \rightarrow \searrow T_m$). Whilst performing well under standard laboratory polymerization conditions, *rac*-Me₂Si(2-Me-4-Ph-Ind)₂ZrCl₂/MMAO showed limited molecular weight and stereo-selectivity capabilities under high temperature (130 – 150 °C) solution process conditions. Although immobilization of *rac*-Me₂Si(2-Me-4-Ph-Ind)₂ZrCl₂ onto silica, allowing it to be used under industrially relevant slurry and gas-phase conditions, led to an active catalyst, it failed to incorporate any functionalized comonomer.

KEYWORDS: Functionalized polypropylene, *rac*-Me₂Si(2-Me-4-Ph-Ind)₂ZrCl₂, *rac*-Me₂Si(Ind)₂ZrCl₂, *rac*-Me₂Si(2-Me-4-Ph-Ind)₂HfCl₂, *rac*-Me₂Si(Ind)₂HfCl₂, 10-undecen-1-ol, reactivity.

INTRODUCTION

Polyolefins form the cheapest and most abundantly used class of all polymers. With only a handful of monomers, materials with a wide variety of properties have been obtained ranging from elastomers to thermoplastics. Even the structurally simple linear polyethylene finds use in a wide range of applications from grocery bags to bullet proof vests or medical implants. Tuning the polymer's topology broadens its potential even more, resulting in for example high temperature resistant thermoplastic elastomers and shape memory materials.¹⁻³ However, one feature all these fantastic materials lack is functionality: polyolefins are aliphatic hydrocarbons that are chemically inert and have a very low surface energy. Combining the polyolefins' excellent mechanical properties with the ability to adhere to other materials is of great interest and significant effort has been directed towards the development of various approaches to produce functionalized polyolefins.⁴⁻⁶

Besides surface modification of polyolefin devices by for example corona- or flame treatment,⁷ polyolefins can be functionalized either by post-reactor or in-reactor functionalization processes.⁸ The post-reactor process typically consists of reactive extrusion using a polyolefin, a functional group to be grafted and typically a radical initiator.⁹ In-reactor functionalization is performed on commercial scale for producing functionalized polyethylenes using the high pressure radical process. Although catalytic in-reactor functionalization of polyolefins is frequently being reported in scientific publications and patents,^{4-6, 10-11} no commercial scale process exists to date.

In-reactor functionalization of polyolefins has been reported in literature using various catalytic approaches. For examples, multi-steps processes consisting of (i) coordinative chain transfer polymerization (CCTP) followed by selective oxidation of the metal carbon bond to produce chain-end functionalized polyolefins,¹²⁻¹³ (ii) copolymerization of olefins with comonomers containing latent reactive groups such as substituted styrenes and its derivatives followed by a post-polymerization functionalization step¹⁴ (iii) random incorporation of electrophile-functionalized comonomers such as borane,¹⁵ and aluminum¹⁶ followed by oxidation and (iv) direct

copolymerization of propylene with nucleophile functionalized comonomers typically passivated with silyl- or aluminum alkyl groups.¹⁷⁻¹⁸ The latter is the most common route and has been proven efficient to produce functionalized polyolefins in lab scale and provides access to a wider range of products with different type and amount of functionality. This approach has been applied to produce copolymers of ethylene or α -olefins with olefin comonomers bearing polar functionalities such as hydroxyls,¹⁹⁻²¹ phenols,²²⁻²³ carboxylic acids,²⁴⁻²⁶ (thio)esters,²⁷ epoxides,²⁸ (thio)ethers²⁹ typically using single-site metallocene catalysts. Recently, unprotected amine and anisyl functionalized monomers have been directly copolymerized with ethylene and propylene using group 3-4 single-site metal-based catalysts to access amine functionalized polyolefins.³⁰⁻³³ Nevertheless, the presence of even small amounts of functionalized comonomers, including the passivated ones, typically have a negative effect on the catalytic activity of the highly electrophilic catalysts. The majority of the studies on functionalized polyolefins are focused on the catalytic performance in the presence of these (passivated) functionalized comonomers (catalytic activity, incorporation ability of functionalized comonomer).³⁴

Since its publication by Spaleck et al. in 1994,³⁵ the unprecedented activity and isospecificity of *rac*-Me₂Si(2-Me-4-Ph-Ind)₂ZrCl₂ (**1**) in propylene polymerization has inspired many researchers to investigate the structure property relationship of metallocenes and **1** has become a benchmark catalyst for many olefin (co)polymerization studies.³⁶⁻³⁸ The “Spaleck catalyst” (**1**) has also been used to produce randomly functionalized polypropylenes.³⁹⁻⁴¹ Most of these publications described the use of **1** as a catalyst to produce functionalized polypropylenes, but little is known about its actual catalytic behavior when used as a catalyst to produce functionalized polyolefins, especially under industrially relevant conditions.

To be able to evaluate the true commercial potential of this catalyst in an in-reactor functionalization process, a thorough study under industrially relevant conditions is required. Specifically, this implies polymerization temperatures in the range of 60 – 90 °C for gas-phase or slurry processes and \geq 130 °C for a solution process

and polymerization times of >10 minutes to an hour, instead of only seconds at room temperature as performed by Cai and coworkers.⁴¹

No data exist on the catalytic performance of other metallocenes in the copolymerization of propylene and polar comonomers (i.e. alkenols) under industrially relevant conditions. Therefore, prior to exploring the potential of **1** for producing functionalized polyolefins under gas-phase or solution process conditions, the performance of **1** was compared with that of other silylene-bridged zirconium- and hafnium-based catalysts: *rac*-Me₂Si(Ind)₂ZrCl₂ (**2**), *rac*-Me₂Si(2-Me-4-Ph-Ind)₂HfCl₂ (**3**) and *rac*-Me₂Si(Ind)₂HfCl₂ (**4**) (Chart 1). The comparison was directed to the effect of catalyst structure and polymerization conditions on catalytic activity, incorporation ability of functionalized comonomer, molecular weight capability and isospecificity.

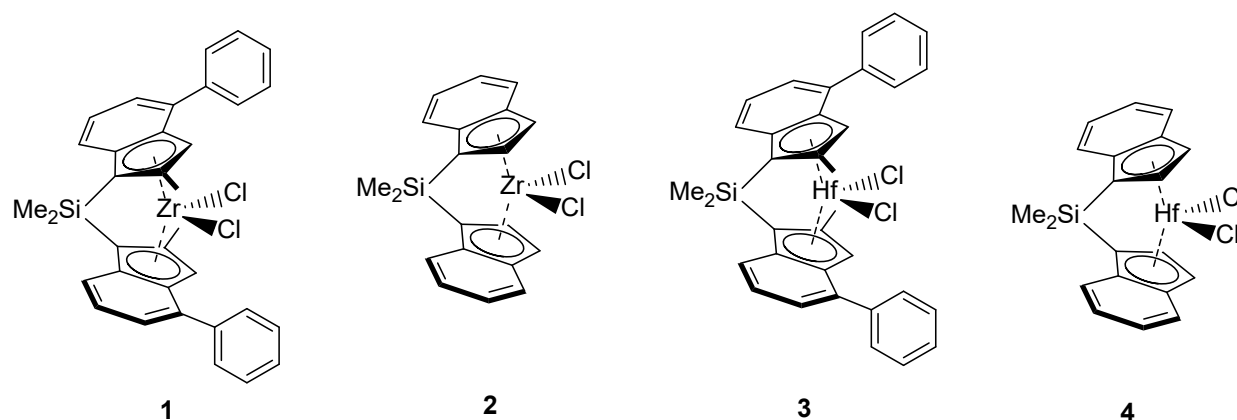


Chart 1. Catalyst precursors used for the copolymerization of propylene/TiBA-passivated 10-undecen-1-ol.

MATERIALS AND METHODS

General considerations. All experiments were performed under an inert dry nitrogen atmosphere using either standard Schlenk or glove box techniques. All chemicals used were purchased from Sigma Aldrich, e.g. MMAO-12 (7 wt% solution in toluene), 10-undecene-1-ol, triisobutylaluminum (TiBA, neat), toluene-HPLC grade and trityl tetrakis(pentafluorophenyl)borate (TB). Propylene was purchased from Abdulla Hashim Gas Co. Saudi Arabia. *rac*-Me₂Si(2-Me-4-Ph-Ind)₂ZrCl₂ (**1**), *rac*-Me₂Si(Ind)₂ZrCl₂ (**2**), *rac*-Me₂Si(2-Me-4-Ph-Ind)₂HfCl₂ (**3**) *rac*-Me₂Si(Ind)₂HfCl₂ (**4**) pre-catalysts were purchased from MCAT GmbH, Germany.

Random copolymerization of propylene and TiBA-passivated 10-undecen-1-ol using 1 – 4 as catalyst precursors. The copolymerization reactions of propylene with TiBA-passivated 10-undecen-1-ol using catalyst precursors **1 – 4** and MMAO-12 “MMAO” as a co-catalyst were performed using a premixed solution of TiBA and C₁₁H₂₁OH (molar ratio of C₁₁H₂₁OH : TiBA 1:1.1) yielding the protonolysis product, C₁₁H₂₁OAl(iBu)₂ (C₁₁H₂₁O-Al(iBu)₂). The copolymerization experiments were carried out in a 0.6 L stainless steel Büchi reactor system (assembled by Hi-Tech, India) equipped with a propeller-like stirrer. The reactor was evacuated and heated using an external oil bath. The reactor vessel was kept under vacuum at a temperature of 110 °C for 10 minutes to remove any condensed moisture. The reactor vessel was then purged with argon and vacuum several times. After this step, the reactor vessel was cooled to the required polymerization temperature. For example entry 2, Table 1, the total volume of the polymerization medium was kept to approx. 200 mL and the reactor was charged with the required amounts of toluene (200 mL)/MMAO-12 (7 wt% solution in toluene, 0.5 mL), TiBA solution (10 wt% solution in toluene, 2.1 mmol) and the solution of C₁₁H₂₁O-Al(iBu)₂ (1 M solution in toluene, 1 mL, 5 mM). The mixture was then pre-saturated with propylene at a pressure of 5 bar and the required polymerization temperature (80 °C). Finally, the catalyst precursor solution in toluene (0.06 μmol) was injected into the reactor vessel applying an overpressure of argon of 0.5 bar. The polymerization started immediately upon the addition of the catalyst precursor. The stirring speed was kept at 500 RPM and the polymerization was performed for 20

minutes. The polymerization temperature was maintained constant during the reaction by circulating hot oil in the reactor jacket and cooling liquid through a cooling spiral inside the reactor vessel. The SCADA software (see supporting information for details) was used to control the reaction temperature and pressure of the polymerization reactor precisely. The propylene consumption was followed using a mass flow controller (MFC) to keep the pressure constant. At the end of the set time, the polymerization was stopped by depressurizing the reactor. The resulting mixture containing the polymer was then quenched with acidified methanol (200 mL, 5 mol% HCl) and subsequently an acetone solution (5 mL) containing butylated hydroxytoluene (2,6-tBu₂-4-Me-C₆H₂OH, BHT) (30 g of BHT in 1 L acetone) was added and the product mixture was stirred for 3 hours. The polymer was then filtered, washed four times with demineralized water, filtered and dried overnight in a vacuum oven at 60 °C to yield 15.2 g of poly(propylene-*co*-undecenol). The functionality content was determined by ¹H NMR and a typical ¹H NMR of poly(propylene-*co*-undecenol) prepared using **1**/MMAO is shown in Figure S4. The relative integrated intensity ratio of the CH₂OH resonances and of methine proton -CH₂CH(CH₃)- resonances of propylene repeating units (1.6 ppm) was used to determine the incorporation of C₁₁OH.

Slurry phase copolymerization of propylene and TiBA-passivated 10-undecen-1-ol using silica supported **1.** A similar polymerization procedure was applied in propylene copolymerization with TiBA-passivated 10-undecen-1-ol catalyzed by the silica-supported *rac*-Me₂Si(2-Me-4-Ph-Ind)₂ZrCl₂ catalyst (**1**):

Gas-phase conditions: 50 mg of silica-supported **1** pre-mixed with paraffin oil (16.7 wt.%), TiBA (1.0 M solution in hexane, 1 mL), propylene pressure = 20 bar, reaction time = 60 min. 10-undecen-1-ol (C₁₁OH), pre-mixed with TiBA (1 M solution in toluene; [TiBA]:[C₁₁OH] = 1.0).

Slurry-phase conditions: 10 mg of silica-supported **1**, heptane (275 mL), TiBA (1.0 M solution in hexane, 1 mL), propylene pressure = 5 bar, reaction time = 40 min. 10-undecen-1-ol (C₁₁OH), pre-mixed with TiBA (1 M solution in toluene; [TiBA]:[C₁₁OH] = 1.0).

The supported catalyst $1/\text{SiO}_2$ was prepared following the conditions described in reference 42.

Analytical Techniques.

High Temperature Size Exclusion Chromatography (HT-SEC). The molar mass and molar mass distribution of the polymers were determined using SEC (PL-GPC 220, Agilent Technologies). The SEC was equipped with two PLgel Olexis 300×7.5 mm columns and the analysis of polymer samples was performed at 160°C . 1,2,4-trichlorobenzene was used as the solvent. BHT (0.0125 wt.%) was added to 1,2,4-trichlorobenzene to prevent the degradation of the polymer samples. A sample solution of approximately $2 \text{ mg}\cdot\text{mL}^{-1}$ was prepared at 170°C using PL-SP260 sample preparation unit equipped with a heater and shaker. A sample volume of $100 \mu\text{L}$ was injected into the SEC columns. The columns were calibrated using narrow mass distribution polystyrene standards using the universal calibration method. The chromatographic data were analyzed using the Agilent GPC/SEC software. The polystyrene-based calibration curve was converted into the universal one using the Mark-Houwink constants of polystyrene ($K = 0.000121 \text{ dL}\cdot\text{g}^{-1}$ and $\alpha = 0.707$) and polypropylene ($K = 0.000135 \text{ dL}\cdot\text{g}^{-1}$ and $\alpha = 0.750$).

Nuclear magnetic resonance spectroscopy (NMR). The samples were dissolved at 130°C in deuterated tetrachloroethane (TCE-d_2) containing BHT as stabilizer. The spectra were recorded in 5 mm tubes on a Bruker Avance 500 spectrometer equipped with a cryogenically cooled probe head operating at 125°C . Chemical shifts are reported in ppm versus the residual solvent protons.

Differential Scanning Calorimetry (DSC). DSC experiments were conducted using a TA DSC Q2000 instrument. The temperature and heat flow of the apparatus were calibrated with an indium standard. For the DSC analysis, the specimens were heated in a nitrogen atmosphere (flow rate $50 \text{ mL}\cdot\text{min}^{-1}$) at $10^\circ\text{C}\cdot\text{min}^{-1}$. A sample of about 5 – 10 mg was used for the experiment and the T_m values were determined from the second heating cycle.

RESULTS AND DISCUSSION

Copolymerization of propylene with $C_{11}^{\bar{O}}\text{-Al}i\text{Bu}_2$ using catalysts **1** – **4**/MMAO

The first series of experiments focused on the optimization of the catalyst loading to operate under isothermal conditions in propylene polymerization. The concentration of **1** had to be lowered to 0.3 μM to achieve well-controlled isothermal propylene polymerization experiments, giving reproducible yields and polymer molecular weights. Due to the inherent deactivation of early transition metal-based catalysts by polar comonomers, the 10-undecen-1-ol ($C_{11}^{\bar{O}}\text{OH}$) had to be passivated with TiBA and the catalyst loading had to be adjusted during propylene/ $C_{11}^{\bar{O}}\text{-Al}i\text{Bu}_2$ copolymerization to produce acceptable amounts of functionalized polypropylenes (vide infra). The effect of co-catalyst type and amount was also investigated and the optimum balance between the catalyst activity and product properties (MW, T_m) was achieved using MMAO co-catalyst (see supp. info. for details).

Attempts to understand the effect of the catalyst structure on its catalytic performance in propylene/ $C_{11}^{\bar{O}}\text{-Al}i\text{Bu}_2$ copolymerization (catalytic activity and copolymer properties), three additional catalyst precursors have been selected based on their structural similarities with **1**: pre-catalyst **2**, which is the unsubstituted bis(indenyl) congener of **1**; complex **3**, which has the same ligand structure as **1** but with hafnium as the metal; complex **4**, which is the unsubstituted bis(indenyl) analogue of **3**. The comparative copolymerizations of propylene and $C_{11}^{\bar{O}}\text{-Al}i\text{Bu}_2$ have been conducted at fixed polymerization temperature (80 °C) and propylene pressure (5 bar) and the results are summarized in Table 1.

Table 1. Results of propylene copolymerization with $C_{11}^{\ominus}O$ -AliBu₂ catalyzed by **1** – **4**/MMAO catalyst systems at 80 °C.^a

run #	Cat.	Cat. μmol	$C_{11}^{\ominus}O$ -AliBu ₂ ^b mM	Yield g	Activity $\text{kg}\cdot\text{mmol cat.}^{-1}\cdot\text{h}^{-1}$	M_n^c $\text{kg}\cdot\text{mol}^{-1}$	\bar{D}^c	T_m^d °C	$C_{11}OH^e$ mol%
1		0.06	0	26.4	1320	80.5	3.0	154.7	0
2	1	0.06	10	15.6	782	127.4	2.3	152.4	0.2
3		0.06	20	5.4	269	162.6	2.4	150.6	0.4
4		0.06	40	5.0	252	127.5	2.8	141.8	0.8
5		0.32	0	21.7	203	12.1	2.3	130.0	0
6	2	0.32	10	16.0	150	14.3	2.4	129.4	0.1
7		0.32	20	13.3	125	14.8	2.3	129.0	0.2
8		0.32	40	11.5	108	15.8	2.3	126.1	0.5
9		1.86	0	9.6	16	40.6	3.3	152.8	0
10	3	1.86	10	8.2	13	40.7	3.1	148.6	0.2
11		1.86	20	6.9	11	43.8	3.2	146.3	0.4
12		1.86	40	7.5	12	45.8	3.1	140.8	0.8
13		1.86	0	14.3	23	69.7	3.2	129.7	0
14	4	1.86	10	12.0	19	44.9	4.9	129.2	0.1
15		1.86	20	11.6	19	82.9	2.6	129.5	0.3
16		1.86	40	7.4	12	54.5	3.5	125.9	0.6

a) Conditions: reactions performed in a 600 mL Büchi reactor, 200 mL toluene, propylene pressure = 5 bar, [MMAO]/[cat. **1**] ~ 8300, [MMAO]/[cat. **2**] ~ 8092, [MMAO]/[cat. **3**] ~ 4284, [MMAO]/[cat. **4**] ~ 4284, TiBA (10 wt% solution in toluene) = 2.1 mmol, reaction time = 20 min. b) 10-undecen-1-ol ($C_{11}^{\ominus}OH$) premixed with TiBA (10 wt% solution in toluene; [TiBA]:[$C_{11}^{\ominus}OH$] = 1.1). c) Determined by HT-SEC in TCB at 160 °C. d) Determined by DSC. e) Determined by ¹H NMR.

At lower $C_{11}=O-Al iBu_2$ feed concentration (up to 10 mM), the catalytic activity of the zirconium based catalysts **1** and **2** is at least an order of magnitude higher than of the hafnium-based analogues **3** and **4**, respectively (Figures 1 A-B). This observation is in line with literature data, commonly reporting higher catalytic activities of zirconocenes than analogous hafnocenes in olefins polymerization.⁴³⁻⁴⁴ Increasing the $[C_{11}=O-Al iBu_2]$ feed concentration (> 10 mM) resulted in a clear negative effect on catalytic activities for all catalysts **1** – **4**, irrespective of the catalyst metal center or ligand structure.

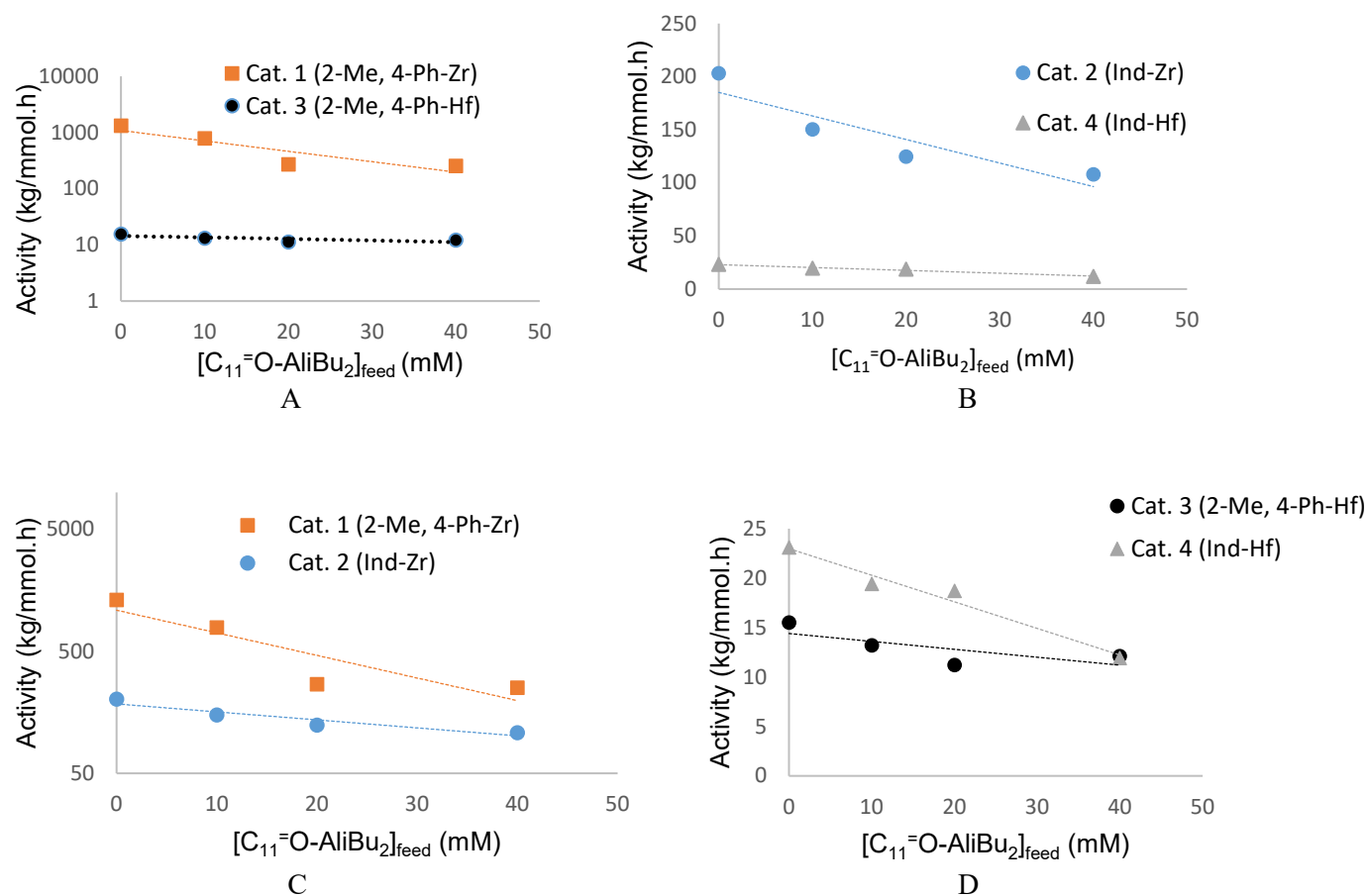


Figure 1. Comparison of the catalytic activity against the feed concentration of $C_{11}=O-Al iBu_2$ in propylene/ $C_{11}=O-Al iBu_2$ copolymerization at 80 °C catalyzed by **1** – **4**/MMAO: (A) metal center effect **1** versus **3**; (B) metal center effect **2** versus **4**; (C) ligand effect **1** versus **2**; (D) ligand effect **3** versus **4**.

This relative drop in catalytic activity seems, however, to be more pronounced for the zirconium-based catalysts **1** and **2**. As a result of its initial higher catalytic activity, the deactivation of **1** seems the strongest but even with the highest feed concentrations of $C_{11}^{\bar{O}}\text{-AliBu}_2$ (40 mM), the catalytic activity of **1** is still significantly higher than for **2–4** during propylene homopolymerization. Comparing the catalytic activity of the reference polymerization experiments for **1–4** with the average catalytic activity for the three last entries for each catalyst where $[C_{11}^{\bar{O}}\text{-AliBu}_2] \geq 20$ mM shows a comparable drop in activity for **2** and **4** (40 – 50 %) and the lowest deactivation was observed using **3** (~ 20 %). The comparison of the ligand effect for **1–4** did not show a distinct trend with overall higher catalytic activities observed using the zirconium-based catalyst bearing the substituted indenyl ligand **1** (Figure 1 C) and the opposite trend was observed with hafnium-based catalysts **3–4** with higher catalytic activity displayed by **4** (Figure 1 D).

The ability of **1 – 4** to incorporate $C_{11}^{\bar{O}}\text{-AliBu}_2$ was analyzed by ^1H NMR and a typical ^1H NMR of poly(propylene-*co*-undecenol) prepared using **1**/MMAO is shown in Figure S4. The methylene protons of the $CH_2\text{OH}$ showed a clear triplet at 3.6 ppm. Plotting the $C_{11}^{\bar{O}}\text{OH}$ content versus the $[C_{11}^{\bar{O}}\text{-AliBu}_2]_{\text{feed}}$ (Figure 2) clearly demonstrates the effect of the catalyst structure on its ability to incorporate $C_{11}^{\bar{O}}\text{-AliBu}_2$. Higher functionality levels were obtained for the zirconocene and hafnocene bearing the substituted indenyl ligand (**1** versus **2**; **3** versus **4**). This is in line with the observed higher α -olefin incorporation during ethylene/ α -olefin copolymerization using substituted bis(indenyl) catalysts versus their unsubstituted analogues.⁴³ During ethylene/ α -olefin copolymerization, hafnocenes typically give a higher α -olefin incorporation than structurally similar zirconocenes.⁴⁵ In our study the effect of the metal is most clearly visible for the unsubstituted metallocenes where hafnocene **4** indeed incorporates $C_{11}^{\bar{O}}\text{-AliBu}_2$ better than the zirconocene **2**. The difference for **1** and **3** is less clear.

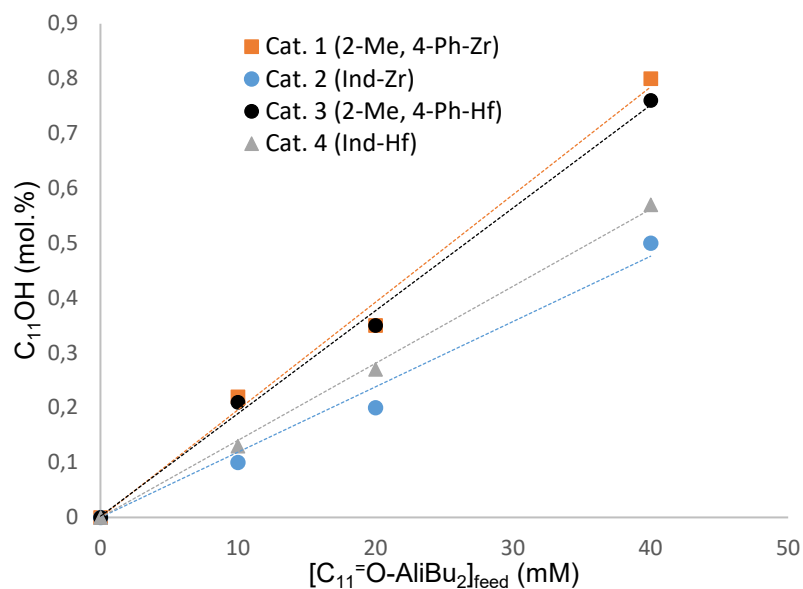


Figure 2. Plot of C₁₁=OH content (mol%) of poly(propylene-*co*-undecenol) copolymers prepared using catalysts **1-4** against the feed concentration of C₁₁=O-AlIBu₂ (mM) at 80 °C.

The plot of the melting temperature versus C₁₁=O-AlIBu₂ feed concentration confirms the efficient incorporation of C₁₁=OH using catalysts **1 – 4** with functionality levels increasing linearly with the increase of C₁₁=O-AlIBu₂ feed concentration at constant propylene concentration, in agreement with the pseudo-first order kinetics of a semi-batch experiment. The effect of the catalyst structure is clearly demonstrated in Figure 3, where the plots of melting temperature against [C₁₁=O-AlIBu₂]_{feed} (Figure 3A) and comonomer content (Figure 3B) obtained using substituted catalysts **1, 3** reveal a clear distinction compared to those obtained using the unsubstituted catalysts **2, 4**. The linear inverse correlation between the melting temperatures and the [C₁₁=O-AlIBu₂]_{feed} is the direct consequence of the first order dependence of the incorporation of C₁₁=O-AlIBu₂ on the C₁₁=O-AlIBu₂ feed concentration, while the difference in the absolute melting temperatures for poly(propylene) and poly(propylene-*co*-undecenol) with the same comonomer

(C_{11}^{OH}) content is caused by the difference in the regio- and stereo-selectivity of catalysts **1** – **4**. This behavior is clearly governed by the steric hindrance imposed by the Me- and Ph- substituents of the indenyl ligand for catalysts **1** and **3** with melting temperatures of about 20 °C higher compared to the samples produced under identical conditions using catalysts **2** and **4** using the same C_{11}^{O} -AliBu₂ feed concentration.

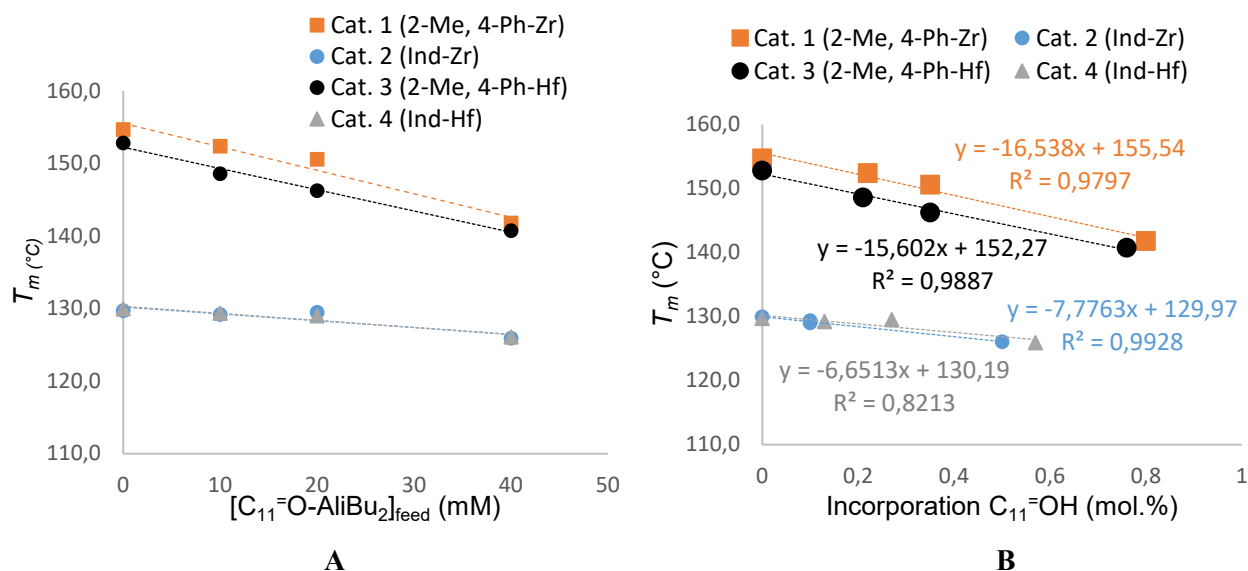


Figure 3. (A) Plot of melting temperature of poly(propylene-*co*-undecenol) copolymers prepared using catalysts **1** – **4** against the feed concentration of C_{11}^{O} -AliBu₂ at 80 °C. (B) Plot of melting temperature of poly(propylene-*co*-undecenol) copolymers prepared using catalysts **1** – **4** against the incorporation of C_{11}^{OH} .

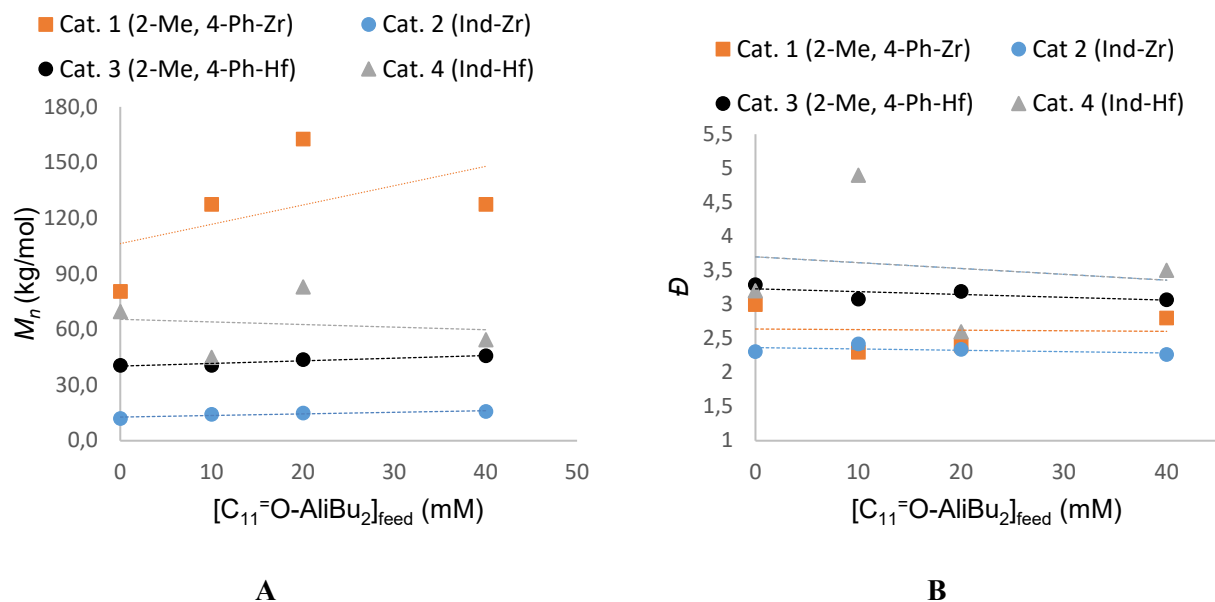


Figure 4. (A) Plot of M_n of poly(propylene-*co*-undecenol) copolymers prepared using catalysts **1** – **4** against the feed concentration of $C_{11}=O-AlIBu_2$ at 80 °C. (B) Plot of D of poly(propylene-*co*-undecenol) copolymers prepared using catalysts **1** – **4** against the feed concentration of $TiBA-C_{11}=OH$ at 80 °C.

The catalyst structure has a clear effect on the polymer molecular weight and the polydispersity index (D). Both catalysts bearing substituted indenyl ligands provide higher molecular weights. This is clearly visible when comparing zirconocenes **1** and **2** with higher molecular weights obtained with the substituted indenyl zirconocene **1** ($M_n > 80$ kg/mol for **1** and $M_n < 20$ kg/mol for **2**). The trend is less pronounced when comparing hafnocene catalysts **3** – **4** (Figure 4). This is in-line with literature reports using these C_2 -symmetric silylene-bridged metallocene catalysts in propylene polymerization and ethylene/propylene copolymerization.^{36,46} Whereas the molecular weight is mainly governed by the ligand structure, the polydispersity is strongly influenced by the choice of the metal. The zirconocenes clearly show a lower D than the isostructural hafnium catalysts (Figure 4B).

Although Figure 3 provides a qualitative picture of the relative ability of **1** – **4** to incorporate $C_{11}^{\text{=O}}$ -AliBu₂, to quantify these results the reactivity ratios have to be determined. The monomer reactivity ratios in propylene/ $C_{11}^{\text{=O}}$ -AliBu₂ copolymerizations were calculated based on the conversions of propylene and $C_{11}^{\text{=OH}}$ and their respective feed concentrations and incorporation in the copolymer (Chart S1). The results of 4 – 5 copolymerization experiments with varying $C_{11}^{\text{=O}}$ -AliBu₂ feed concentrations were used to determine the value of the reactivity ratio r_1 applying the following linear methods:^{47,48}

$$(1) \quad r_1 = \frac{C_3 \text{ conv.} (C_{11}^{\text{OH}} \text{ conv.} - 1)}{C_{11}^{\text{OH}} \text{ conv.} (C_3 \text{ conv.} - 1)}$$

$$(2) \quad r_1 \frac{[C_{11}^{\text{=O}}\text{-Al}^i\text{Bu}_2]_{\text{copol}}}{[C3]_{\text{copol}}} = \frac{[C_{11}^{\text{=O}}\text{-Al}^i\text{Bu}_2]_{\text{feed}}}{[C3]_{\text{feed}}}$$

$$(3) \quad r_1 \frac{F^2}{f} = \frac{F(f-1)}{f} \quad \text{where} \quad F = \frac{[C3]_{\text{feed}}}{[C_{11}^{\text{=O}}\text{-Al}^i\text{Bu}_2]_{\text{feed}}} \quad \text{and} \quad f = \frac{[C3]_{\text{copol}}}{[C_{11}^{\text{=O}}\text{-Al}^i\text{Bu}_2]_{\text{copol}}}$$

The reactivity ratios calculated using methods 1 – 3 are listed in Table 2 and plotted in Figure 5. Interestingly, regardless of the method employed (Table 2), the r_1 's shows the following order: r_1 (**2**) > r_1 (**4**) > r_1 (**3**) ~ r_1 (**1**). This order clearly indicates the influence of the ligand structure on the relative reactivity of propylene and $C_{11}^{\text{=O}}$ -AliBu₂ with lower reactivity ratios obtained with the catalysts bearing the substituted indenyl ligands **1** and **3** as compared to **2** and **4**, respectively. This is in agreement with the behavior of substituted bis(indenyl) metallocene catalysts in ethylene – α -olefins copolymerizations.⁴³ Furthermore, the effect of the catalyst's metal center seems

to be visible only when comparing the unsubstituted indenyl complexes **2** and **4** with a higher comonomer reactivity displayed by the hafnocene catalyst **4**.

Table 2. Summary of the reactivity ratios for catalysts **1** – **4** obtained using methods 1 – 3 in propylene copolymerization with $C_{11}^-O-AliBu_2$ at 80 °C.

Cat.	$[C_{11}^-O-AliBu_2]_{feed}$	Average reactivity ratio r_1		Method 3 ⁴⁷ reactivity ratio r_1
		Method 1 ⁴⁶	Method 2 ⁴⁶	
1	10	2.4 ± 0.4	1.8 ± 0.2	1.5
	20			
	30			
	40			
2	10	6.5 ± 1.7	3.3 ± 0.4	3.3
	20			
	30			
	40			
3	10	2.3 ± 0.2	1.9 ± 0.2	1.6
	20			
	30			
	40			
4	10	4.0 ± 0.7	2.6 ± 0.1	2.8
	20			
	30			
	40			

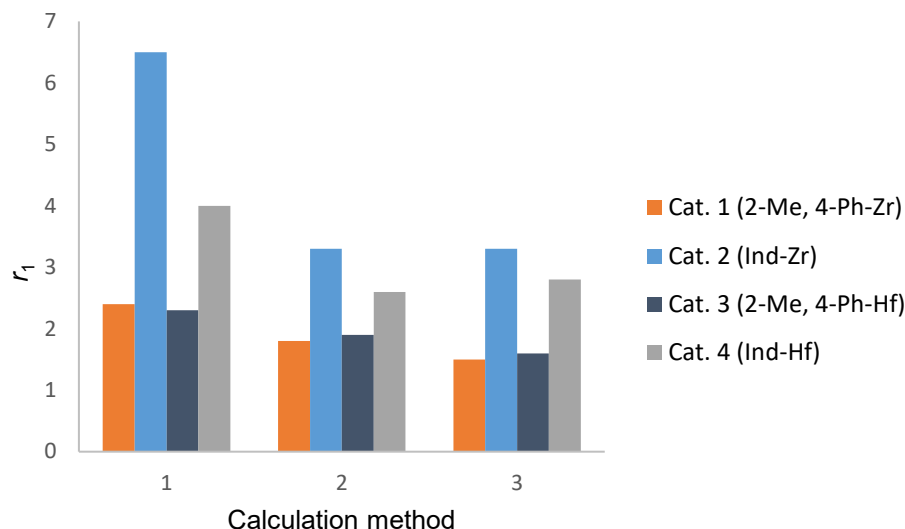


Figure 5. Plot of reactivity ratio r_1 in propylene copolymerization with $C_{11}^{\text{=O}}\text{-Al}i\text{Bu}_2$ obtained at 80 °C with catalysts **1** – **4**/MMAO determined using methods 1-3. See Table 2 for details.

Copolymerization of propylene with $C_{11}^{\text{=O}}\text{-Al}i\text{Bu}_2$ using **1**/MMAO at 40 – 100 °C.

Based on the comparison of catalytic performance of **1** – **4**, zirconocene **1** bearing the substituted 2-Me, 4-Ph indenyl ligand clearly stands out as the best performing catalyst in propylene – $C_{11}^{\text{=O}}\text{-Al}i\text{Bu}_2$ copolymerization with higher catalytic activity, higher molecular weight capability, enhanced stereo-selectivity and reactivity towards $C_{11}^{\text{=O}}\text{-Al}i\text{Bu}_2$ comonomer (a lower r_1 value). Hence, the focus of the rest of this study was directed towards **1**/MMAO as the catalyst system to evaluate its behavior at different temperatures and using different $C_{11}^{\text{=O}}\text{-Al}i\text{Bu}_2$ feed concentrations. The copolymerization results are presented in Table 3 and Figure 6. In the range of polymerization temperatures from 40 to 90 °C, the catalytic activity gradually increased with increasing temperature. Increasing the temperature further to 100 °C resulted in a drop of catalytic activity. Keeping in mind that with increasing temperature from 40 to 100 °C at constant propylene pressure, the concentration of the dissolved propylene significantly drops (the ratio $[C_3^{\text{=}}]_{100\text{ °C}}/[C_3^{\text{=}}]_{40\text{ °C}} \approx 0.4$, as determined using Peng-

Robinson equation of state with properties parameters from Aspen Plus[®]), the actual rate constant of the polymerization will increase approx. with a factor of 2.5 more than the observed activity obtained under the same propylene pressure. The observed activity at 100 °C was lower than expected, which is either the result of mass transfer limitation at this temperature—meaning that the propylene consumption rate exceeds the propylene dissolution rate—or the result of thermal decomposition of the catalyst. For each polymerization temperature, the catalytic activity is inversely proportional to the C₁₁=O-AliBu₂ feed concentration (Figure 6A). This is in agreement with the hypothesis that the oxygen of the C₁₁=O-AliBu₂ is still capable to weakly and reversibly coordinate to the highly electrophilic active center. The thus obtained equilibrium of active and dormant catalyst species shifts to the side of dormant species with an increasing concentration of C₁₁=O-AliBu₂ in the system.

Table 3. Results of propylene copolymerization with C₁₁=O-AliBu₂ using 1/MMAO as catalyst system at variable polymerization temperatures. ^a

run #	C ₁₁ =O-AliBu ₂ ^b mM	T °C	Yield g	Activity kg·mmol cat. ⁻¹ ·h ⁻¹	M _n ^c kg·mol ⁻¹	<i>D</i> ^c	T _m ^d °C	C ₁₁ OH ^e mol%
1	0	40	0.9	48	617.3	2.5	160.2	0
2	10	40	2.5	127	872.5	2.0	157.6	0.10
3	20	40	2.1	105	1121.0	1.8	155.5	0.20
4	30	40	2.4	119	1012.0	1.9	154.5	0.32
5	40	40	1.7	85	1008.0	1.9	151.0	0.50
6	0	60	19.9	993	132.1	3.2	158.3	0
7	10	60	6.8	338	454.4	2.1	156.3	0.10
8	20	60	4.3	216	464.4	2.0	152.8	0.38
9	30	60	3.8	191	443.3	2.1	151.5	0.43
10	40	60	2.7	137	441.4	2.2	147.7	0.90

11	0	70	21.8	1090	98.9	3.4	156.8	0
12	10	70	6.0	298	316.6	2.1	154.8	0.20
13	20	70	6.3	315	273.9	2.2	152.2	0.35
14	30	70	3.5	177	275.4	2.2	148.9	0.65
15	40	70	4.1	203	218.2	2.7	147.0	1.00
16	0	80	26.4	1320	80.5	3.0	154.7	0
17	10	80	15.6	782	127.4	2.3	152.4	0.22
18	20	80	5.4	269	162.6	2.4	150.6	0.36
19	30	80	5.8	289	149.9	2.5	146.6	0.70
20	40	80	5.0	252	127.5	2.8	141.8	0.80
21	0	90	26.8	1340	61.7	2.5	154.0	0
22	10	90	19.6	981	63.5	2.7	150.9	0.25
23	20	90	14.9	747	76.5	2.4	148.0	0.40
24	30	90	7.5	374	78.0	2.4	144.8	0.70
25	40	90	3.8	190	77.3	2.5	141.6	0.85
26	0	100	23.4	1170	36.7	2.6	150.0	0
27	10	100	14.7	733	44.7	2.4	148.0	0.25
28	20	100	10.8	535	44.8	2.5	144.8	0.50
29	30	100	5.1	255	46.8	2.5	141.9	0.70
30	40	100	2.6	130	46.0	2.5	138.0	1.05

a) Conditions: reaction performed in a 600 mL Büchi reactor, 200 mL toluene, propylene pressure = 5 bar, [MMAO]/[cat. **1**] ~ 8300, TiBA (10 wt% solution in toluene) = 2.1 mmol, reaction time = 20 min, cat. **1** = 0.06 μ mol. b) 10-undecen-1-ol ($C_{11}OH$) premixed with TiBA (10 wt% solution in toluene; [TiBA]/[$C_{11}OH$] = 1.1). c) Determined by HT-SEC in TCB at 160 °C. d) Determined by DSC. e) Determined by 1H NMR.

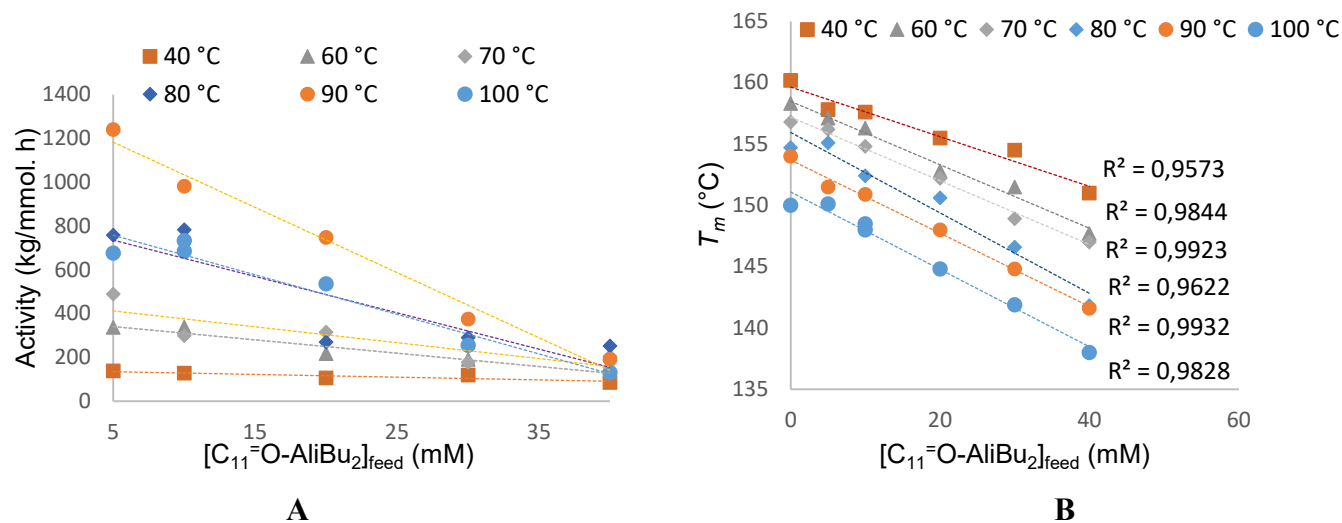


Figure 6. Plots of (A) catalytic activities and (B) melting temperatures of poly(propylene-*co*-undecenol) of 1/MMAO against the feed concentration of C₁₁=O-AlIBu₂ (mM) at variable polymerization temperatures.

The synthesized copolymers at different temperatures were characterized using DSC thermal analysis, HT-SEC chromatography and ¹H NMR spectroscopy. The DSC data are presented in Table 3 and plotted in Figure 6 B and the individual DSC thermographs are presented in Figures S6 – S11. The melting temperature development of poly(propylene-*co*-undecenol) against the feed concentration of C₁₁=O-AlIBu₂ at polymerization temperatures ranging from 40 to 100 °C shows a linear inversely proportional relationship, which is in line with first order kinetics and provides clear evidence of the increased incorporation of the C₁₁=OH comonomer with increasing C₁₁=O-AlIBu₂ feed concentration. This was confirmed by ¹H NMR analysis showing a linear relationship between C₁₁=OH incorporation and its initial feed concentration (Table 3, Figure 7A). The fact that the C₁₁=O-AlIBu₂ incorporation increases with increasing polymerization temperature (Figure 7A) can be explained by the decreasing propylene concentration (higher C₁₁=O-AlIBu₂ /propylene ratio) upon increasing the polymerization temperature while keeping the propylene pressure constant.

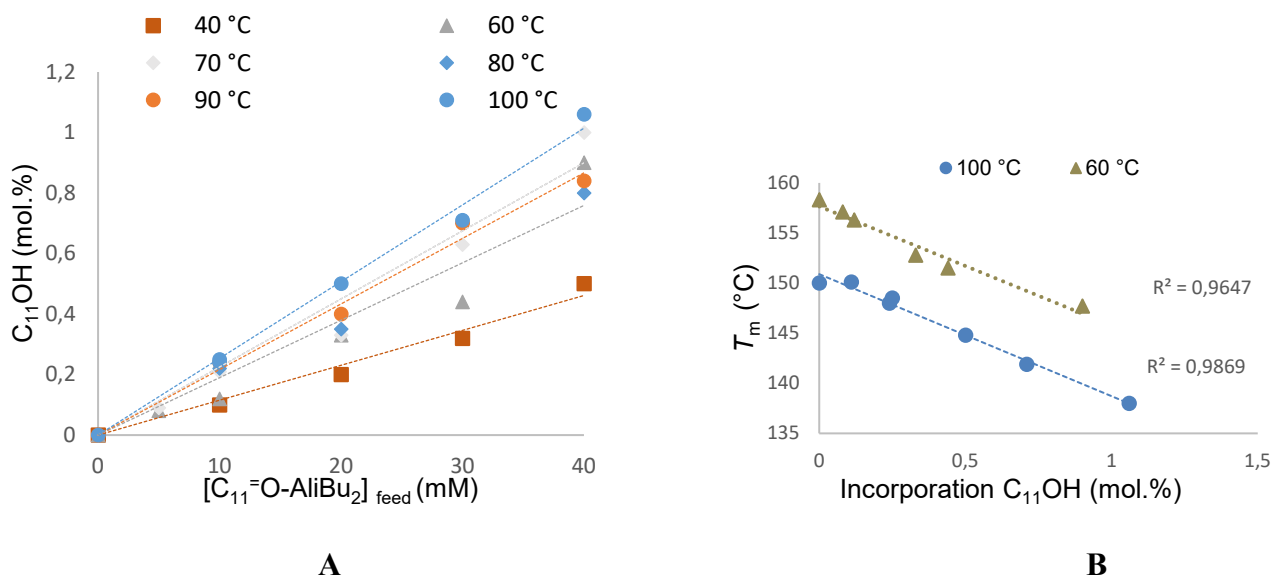


Figure 7. (A) Plot of $C_{11}OH$ incorporation (mol%) against the feed concentration of $C_{11}O-AliBu_2$ (0 – 40 mM). (B) Plot of the melting temperatures of poly(propylene-*co*-undecenol) against the $C_{11}OH$ content (mol%) in copolymers produced at 60 and 100 °C.

Furthermore, the melting temperatures of poly(propylene-*co*-undecenol) copolymers listed in Table 3 were plotted against the comonomer content determined by 1H NMR (Figure 7B). The inverse linear correlations (T_m versus $C_{11}OH$ content) of the samples produced at 60 and 100 °C show similar slope (~ -12), which indicate a linear dependency of the melting temperatures of poly(propylene-*co*-undecenol) on comonomer content irrespective of the polymerization temperature. The difference in the absolute T_m values for homopolymers or copolymers containing the same amount of $C_{11}OH$ (mol%) produced at 60 and 100 °C of approx. 8 °C results from the difference in stereo/region errors occurring at increasing extent when increasing the polymerization temperature.

The HT-SEC analysis of the copolymers produced at different temperatures and $C_{11}O-AliBu_2$ feed concentrations showed that the amount of $C_{11}O-AliBu_2$ in the feed has no effect on the copolymer's

molecular weight whereas the increase in polymerization temperature resulted in a significant drop of poly(propylene-*co*-undecenol) molecular weight (Figure 8). The latter can be explained by the decreasing propylene concentration (at a fixed propylene pressure of 5 bar) and the decreasing $\Delta E_{\text{activation}}$ between chain transfer and chain growth with increasing temperature.

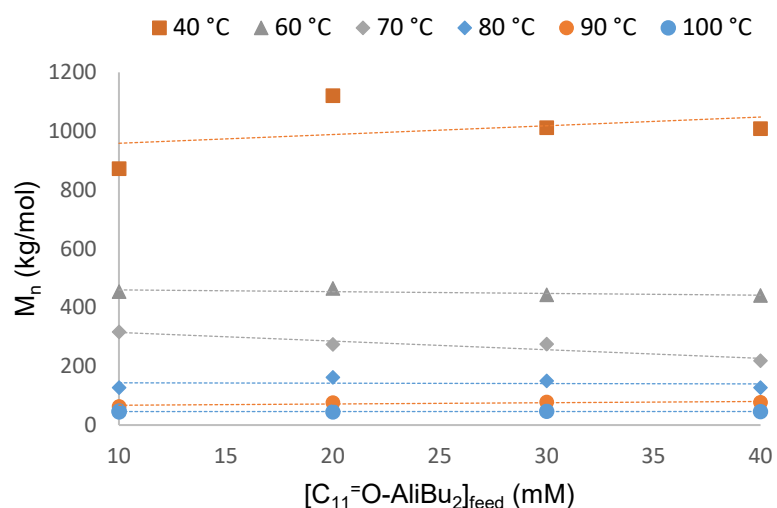


Figure 8. Plots of M_n ($\text{kg}\cdot\text{mol}^{-1}$) of poly(propylene-*co*-undecenol) copolymers produced using **1**/MMAO versus $\text{C}_{11}=\text{O}-\text{Al}i\text{Bu}_2$ feed concentration (mM) at variable polymerization temperatures.

To allow a meaningful comparison of the polymerization data obtained using **1**/MMAO at variable temperatures, the reactivity ratio of propylene and $\text{C}_{11}=\text{O}-\text{Al}i\text{Bu}_2$ was calculated using methods 1 – 3 at corrected propylene concentrations determined using Peng-Robinson equation of state with properties parameters from Aspen Plus[®] versus the polymerization temperatures (Table 4 and Figure 9). From Figures 9, it is evident that the polymerization temperature has a significant effect on the reactivity ratio of propylene/ $\text{C}_{11}=\text{O}-\text{Al}i\text{Bu}_2$ with a steady drop of r_1 as a function of polymerization temperature indicating that catalyst **1** has an increasing reactivity towards $\text{C}_{11}=\text{O}-\text{Al}i\text{Bu}_2$ comonomer upon increasing polymerization temperature. This can be explained by the

decreasing $\Delta E_{\text{activation}}$ for the insertion reaction of $\text{C}_{11}^{\text{=O-AliBu}_2}$ versus propylene with increasing polymerization temperature, which is in-line with literature reports describing the same behavior of metallocene catalysts in ethylene/ α -olefins⁴³ and ethylene/alkenols copolymerization.⁴⁹

Table 4. Summary of reactivity ratios for catalyst 1/MMAO obtained using methods 1-3 in propylene copolymerization with $\text{C}_{11}^{\text{=O-AliBu}_2}$ using the corrected propylene concentrations derived from Aspen Plus® at six polymerization temperatures 40 to 100 °C.

Temperature	Average reactivity ratio r_1		Method 3 reactivity ratio r_1
	Method 1	Method 2	
40	3.4 ± 0.4	3.2 ± 0.3	2.8
60	2.7 ± 1.3	2.3 ± 0.9	2.7
70	1.9 ± 0.4	1.7 ± 0.3	1.7
80	2.2 ± 0.5	1.7 ± 0.2	1.6
90	2.1 ± 1.0	1.6 ± 0.2	1.5
100	1.8 ± 0.3	1.5 ± 0.1	1.4

^a $[\text{C}_{11}^{\text{=O-AliBu}_2}]_{\text{feed}} = 10, 20, 30 \text{ and } 40 \text{ mM}$.

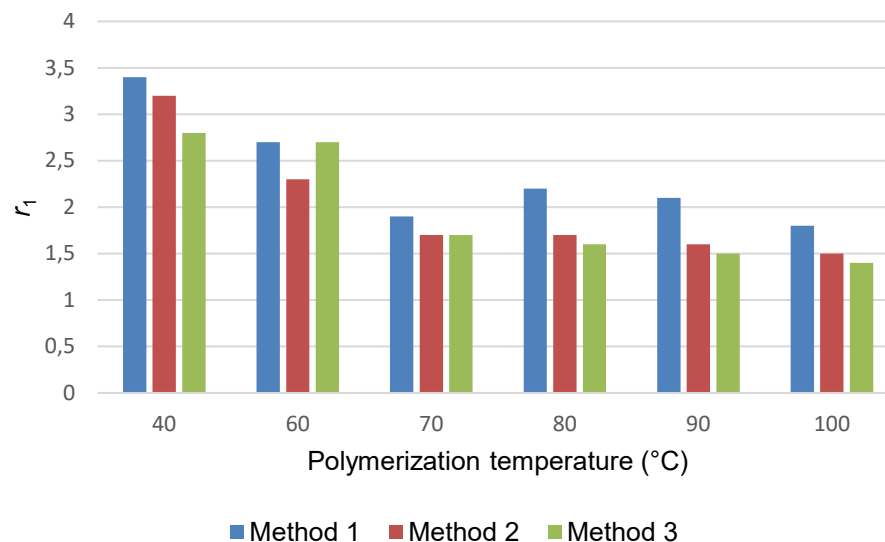


Figure 9. Plot of reactivity ratio r_1 in propylene/ $C_{11}OH$ - $Al(i)Bu_2$ copolymerization catalyzed by **1**/MMAO obtained with corrected propylene concentrations at six different temperatures ranging from 40 to 100 °C using methods 1-3.

To evaluate the potential of **1** in producing hydroxyl-functionalized polypropylenes under industrially relevant process conditions, the performance of **1** in propylene copolymerization with hydroxyl-functionalized α -olefins was carried out under solution process conditions (130-150 °C) and under slurry- and gas-phase process conditions (85 °C) using a silica-supported version of **1**. The silica-supported catalyst **1** was first used in gas-phase propylene copolymerization with 10-undecen-1-ol ($C_{11}OH$) premixed with an equimolar amount of TiBA and the corresponding results are listed in Table S4. Acceptable tolerance to TiBA-passivated 10-undecen-1-ol can be observed and high molecular weight products were obtained ($M_n > 50$ kg/mol). However, DSC and NMR analysis did not show any evidence of $C_{11}OH$ incorporation with melting temperatures comparable to reference polypropylene homopolymer. This was first accredited to the reduced volatility of TiBA-passivated $C_{11}OH$ under the gas-phase reaction conditions, however, the copolymerization trials conducted using the same silica-

supported catalyst under slurry-phase conditions in propylene/ $C_{11}^{\text{=O}}\text{-Al}i\text{Bu}_2$ copolymerization resulted in the same outcome. The lack of affinity or incorporation ability of this silica-supported catalyst towards $\text{TiBA}-C_{11}^{\text{=O}}\text{OH}$, combined with the absence of catalyst poisoning, suggests that $C_{11}^{\text{=O}}\text{-Al}i\text{Bu}_2$ is too sterically hindered to migrate to the active sites of the heterogeneous catalyst and/or is effectively adsorbed onto the catalyst support. Unfortunately, attempts using non-porous solid MAO (Tosoh Finechem Corporation) as support did not lead to better results and replacing TiBA with trimethyl aluminium to afford the less sterically hindered $C_{11}^{\text{=O}}\text{-AlMe}_2$ resulted in catalyst deactivation. To elucidate the exact cause of the lack of incorporation of $C_{11}^{\text{=O}}\text{-Al}i\text{Bu}_2$ once silica supported **1** is applied, an in-depth study requiring dedicated methods and expertise (e.g. surface science, computational methods, etc.) has to be conducted, which falls outside the scope of this paper.

Next, the performance of the unsupported catalyst **1**/MAO was evaluated at 130 – 150 °C in propylene copolymerization with $C_{11}^{\text{=O}}\text{-Al}i\text{Bu}_2$. The propylene polymerization conducted with $C_3^{\text{=}}$ pressures of 5 and 15 bar (to compensate for the lower solubility of propylene at higher temperatures) results indicate clearly the limited molecular weight capability and stereo-selectivity of catalyst **1** at elevated temperatures with $M_n \leq 5$ kg/mol (5 bar $C_3^{\text{=}}$) and ≤ 20 kg/mol (15 bar $C_3^{\text{=}}$) and T_m 's far below those obtained at 80 °C (Table S5). While being a suitable catalyst for lab screening, catalyst **1** shows severe limitations under industrially relevant process conditions.

CONCLUSIONS

This study demonstrates the effect of the catalyst structure and polymerization temperature on the catalytic performance of C_2 -symmetric silylene-bridged zirconocenes and hafnocenes during the copolymerization of propylene and TiBA-passivated 10-undecen-1-ol. The kinetic study revealed a noticeable influence of the



catalyst's metal center with higher catalytic activities obtained using the zirconocenes (**1**, **2**) than analogous hafnocenes (**2**, **4**) during propylene/ $C_{11}O$ -Al_iBu₂ copolymerization. It was found that the substituted indenyl zirconocene (**1**) and hafnocene (**3**) catalysts afford higher comonomer reactivity and stereo-selectivity compared to their non-substituted congeners (**2**, **4**). As expected, a linear relationship between the polymerization temperature versus copolymer molecular weight and melting temperature exists. More importantly, the highly active and iso-selective zirconocene catalyst **1** exhibited an outstanding ability to incorporate the hydroxyl-functionalized α -olefin with an increasing comonomer reactivity upon increasing polymerization temperature, making **1** a catalyst of choice for producing functionalized polyolefins.

On the other hand, the polypropylene functionalization study conducted using this outstanding catalyst under industrially relevant gas-phase and solution process conditions revealed its limited potential to be used as a catalyst for producing hydroxyl-functionalized polypropylene applying the existing polyolefin commercial process technologies with the lack of functionality under gas-phase conditions and limited molecular weight capability and stereo-selectivity at elevated temperatures required in a solution process.

SUPPORTING INFORMATION

The supporting information contains the optimization of propylene polymerization conditions using pre-catalyst $rac\text{-Me}_2\text{Si}(2\text{-Me-4-Ph-Ind})_2\text{ZrCl}_2$ (**1**), Tables listing additional polymerization experiments and Figures showing plots of polymerization activities, MW, T_m , activation energy, DSC thermographs, NMR spectra and reactivity ratios.

ACKNOWLEDGEMENT

The authors would like to acknowledge the support provided by SABIC for funding the project # CRP02278 at Center for Refining and Advanced Chemicals (CRAC)/RI-KFUPM. The support of King Fahd University of Petroleum & Minerals (KFUPM), Dhahran, Saudi Arabia, is also highly appreciated.

AUTHOR INFORMATION

*E-mail for M.B.: Miloud.Bouyahyi@SABIC.com, R.D.: Rob.Duchateau@SABIC.com and M.N.A.: mnakhtar@kfupm.edu.sa

REFERENCES

1. IHS Market. *Polypropylene Edition 2017, 2018*.
2. Hustad, P, D. Frontiers in Olefin Polymerization: Reinventing the World's Most Common Synthetic Polymers. *Science* **2009**, 325, 704–707.
3. Roettger, M.; Domenech, T.; van der Weegen, R.; Breuillac, A.; Nicolay, R.; Leibler, L. High Performance Vitrimers from Commodity Thermoplastics through Dioxaborolane Metathesis. *Science* **2017**, 356, 62–65.
4. Amin, S, B.; Marks, T, J. Versatile Pathways for In Situ Polyolefin Functionalization with Heteroatoms: Catalytic Chain Transfer. *Angew. Chem. Int. Ed.* **2008**, 47, 200–2025.
5. Chung, T. C. Functionalisation of Polyolefins; *Academic Press: London*, **2002**.
6. Franssen, N. M. G.; Reek, J. N. H.; de Bruin, B. Synthesis of Functional Polyolefins: State of the Art and Remaining Challenges. *Chem. Soc. Rev.* **2013**, 42, 5809–5832.
7. Peacock, A. J. Handbook of Polyethylene, Structure, Properties and Applications. Marcel Dekker, Inc **2000**.

8. Boen, N. K.; Hillmyer, M. A. Post-Polymerization Functionalization of Polyolefins *Chem. Soc. Rev.* **2005**, *34*, 267–275.
9. Moad, G. The Synthesis of Polyolefin Graft Copolymers by Reactive Extrusion. *Prog. Polym. Sci.* **1999**, *24*, 81–142.
10. Boffa, L. S.; Novak, B. M. Copolymerization of Polar Monomers with Olefins using Transition-Metal Complexes. *Chem. Rev.* **2000**, *100*, 1479–1493.
11. Dong, J. Y.; Hu, Y. Design and Synthesis of Structurally Well-Defined Functional Polyolefins via Transition Metal-Mediated Olefin Polymerization Chemistry. *Coord. Chem. Rev.* **2006**, *250*, 47–65.
12. Fan, G.; Dong, J-Y. An Examination of Aluminum Chain Transfer Reaction in *rac*-Me₂Si[2-Me-4-Naph-Ind]₂ZrCl₂/MAO-catalyzed Propylene Polymerization and Synthesis of Aluminum-terminated Isotactic Polypropylene with Controlled Molecular Weight. *J. Mol. Cat. A: Chem.* **2005**, *236*, 246–252.
13. Ring, O. J.; Thomann, R.; Mulhaupt, R.; Raquez, J-M.; Degée, P.; Dubois, P. Controlled Synthesis and Characterization of Poly[ethylene-block-(L,L-lactide)]s by Combining Catalytic Ethylene Oligomerization with “Coordination-Insertion” Ring-Opening Polymerization. *Macromol. Chem. Phys.* **2007**, *208*, 896–902.
14. For example, see: Kay, C. J.; Goring P. D.; Burnett, C. A.; Hornby, B.; Lawtas, K.; Morris, S.; Morton, C.; McNally, T.; Theaker, G. W.; Waterson, C.; Wright P. M.; Scott, P. Polyolefin–Polar Block Copolymers from Versatile new Macromonomers. *J. Am. Chem. Soc.* **2018**, *140*, 13921–13934.
15. For example, see: Chung, T. C.; Lu, H. L. Functionalization and Block Reactions of Polyolefins using Metallocene Catalysts and Borane Reagents. *J. Mol. Cat. A: Chem.* **1997**, *115*, 115–127.
16. For example, see: Shiono, T.; Sugimoto, M.; Hasan, T.; Cai, Z. Facile Synthesis of Hydroxy-Functionalized Cycloolefin Copolymer Using ω -Alkenylaluminium as a Comonomer. *Macromol. Chem. Phys.* **2013**, *214*, 2239–2244.

17. For example, see: Goretzki, R.; Fink, G. Homogeneous and Heterogeneous Metallocene/MAO-catalyzed Polymerization of Trialkylsilyl-protected Alcohols. *Macromol. Rapid Commun.* **1999**, *19*, 511–515.
18. Hakala, K.; Helaja, T.; Lofgren, B. Metallocene/methyl aluminoxane-catalyzed Copolymerizations of Oxygen-functionalized Long-chain Olefins with Ethylene. *J. Polym. Sci., Part A: Polym. Chem.* **2000**, *38*, 1966–1977.
19. For example, see: Goretzki, R.; Fink, G. Homogeneous and Heterogeneous Metallocene/MAO-Catalyzed Polymerization of Functionalized Olefins. *Macromolecules Chem. Phys.* **1999**, *200*, 881–886.
20. Aaltonen, P.; Lijfgren, B. Synthesis of Functional Polyethylenes with Soluble Metallocene/Methylaluminoxane Catalyst. *Macromolecules* **1995**, *28*, 5353–5357.
21. Bouyahyi, M.; Turki, Y.; Tanwar, A.; Jasinska J-W.; Duchateau, R. Randomly Functionalized Polyethylenes: In Quest of Avoiding Catalyst Deactivation. *ACS Catal.* **2019**, *9*, 7779–7790.
22. Wilen C-E.; Luttkhedde, H.; Hjertberg, T.; Nasman, J, H. Copolymerization of Ethylene and 6-tert-Butyl-2-(1,1-dimethylhept-6-enyl)-4-methylphenol over Three Different Metallocene-Alumoxane Catalyst Systems. *Macromolecules* **1996**, *29*, 8569–8575.
23. Dong, J, Y.; Chung, T. C. M. Synthesis of Polyethylene Containing a Terminal p-Methylstyrene Group: Metallocene-Mediated Ethylene Polymerization with a Consecutive Chain Transfer Reaction to p-Methylstyrene and Hydrogen. *Macromolecules* **2002**, *35*, 1622–1631.
24. Yang, X-H.; Liu, C-R.; Wang, C.; Sun, X-L; Guo, Y-H; Wang, X-K.; Wang, Z.; Xie, Z.; Tang, Y. [ONSR]TiCl₃-Catalyzed Copolymerization of Ethylene with Functionalized Olefins. *Angew. Chem. Int. Ed.* **2009**, *48*, 8099–8102.
25. Hakala, K.; Lofgren, B.; Helaja, T. Copolymerizations of Oxygen-Functionalized Olefins with Propylene using Metallocene/Methylaluminoxane Catalyst. *Eur. Polym.* **1998**, *34*, 1093–1097.

26. Marques, M, M.; Correia, S, G.; Ascenso, J, R.; Ribeiro, A, F, G.; Gomes, P, T.; Dias, A, R.; Foster, P.; Rausch, M, D.; Chien, J, C. W. Polymerization with TMA-Protected Polar Vinyl Comonomers. I. Catalyzed by Group 4 Metal Complexes with η^5 -type Ligands. *J. Polym. Sci. Part A: Polym. Chem.* **1999**, *37*, 2457–2469.
27. Song, S.; Zhang, Z.; Liu, X.; Fu, Z.; Xu, Z.; Fan, Z. Synthesis and Characterization of Functional Polyethylene with Regularly Distributed Thioester Pendants via Ring-Opening Metathesis Polymerization. *J. Pol. Sci. Part A: Pol. Chem.* **2017**, *55*, 4027–4036.
28. For example, see: Morishita, H.; Sudo, A.; Endo, T. Synthesis and Palladium-Catalyzed Addition Polymerization of Norbornene Carrying Epoxy Moiety. *J. Polym. Sci. Part A: Polym. Chem.* **2009**, *47*, 982–389.
29. Kwasny, T, M.; Watkins, C, M.; Posey, D, N.; Matta, E, M.; Tew, N, J. Functional Polyethylenes with Precisely Placed Thioethers and Sulfoniums through Thiol–Ene Polymerization Comonomers. *Macromolecules* **2018**, *51*, 4280–4289.
30. Shang, R.; Gao, H.; Luo, F.; Li, Y.; Wang, B.; Ma, Z.; Pan, L.; Li, Y. Functional Isotactic Polypropylenes via Efficient Direct Copolymerizations of Propylene with Various Amino-Functionalized α -Olefins. *Macromolecules* **2019**, *52*, 9280–9290.
31. Huang, M.; Chen, J.; Wang, B.; Huang, W.; Chen, H.; Gao, Y.; Marks, T, J. Polar Isotactic and Syndiotactic Polypropylenes via Organozirconium-Catalyzed Masking-Reagent-Free Propylene and Amino-Olefin Copolymerization *Angew. Chem. Int. Ed.* **2020**, *59*, 20522–20528.
32. Chen, J.; Gao, Y.; Wang, B.; Lohr, T, L.; Marks, T, J. Scandium-Catalyzed Self-Assisted Polar Co-monomer Enchainment in Ethylene Polymerization. *Angew. Chem. Int. Ed.* **2017**, *56*, 15964–15968.
33. Wang, C.; Luo, G.; Nishiura, M.; Song, G.; Yamamoto, A.; Luo, Y.; Hou, Z. Heteroatom-assisted Olefin Polymerization by Rare-Earth Metal Catalysts. *Sci. Adv.* **2017**, *3*, e1701011/1-e1701011/8.

34. For example, see: Zhang, X.; Chen, S.; Li, H.; Zhang, Z.; Lu, Y.; Wu, C.; Hu, Y. Copolymerizations of Ethylene and Polar Comonomers with Bis(phenoxyketimine) Group IV Complexes: Effects of the Central Metal Properties. *J. Pol. Sci. Part A: Pol. Chem.* **2006**, *45*, 59–68.
35. Spaleck, W.; Kueber, F.; Winter, A.; Rohrmann, J.; Bachmann, B.; Antberg, M.; Dolle, V.; Paulus, E. F. The Influence of Aromatic Substituents on the Polymerization Behavior of Bridged Zirconocene Catalysts. *Organometallics* **1994**, *13*, 954–936.
36. Ehm, C.; Vittoria, A.; Goryunov, J. P.; Izmer, V. V.; Kononovich, D. S.; Kulyabin, P. S.; Di Girolamo, R.; Budzelaar, P. H. M.; Voskoboynikov, A. Z.; Busico, V. Cipullo, R. A Systematic Study of the Temperature-Induced Performance Decline of ansa-Metallocenes for iPP. *Macromolecules* **2020**, *53*, 9325–9336.
37. Desert, X.; Proutiere, F.; Welle, A.; Den Dauw, K.; Vantomme, A.; Miserque, O.; Brusson, J-M.; Carpentier, J-F.; Kirillov, E. Zirconocene-Catalyzed Polymerization of α -Olefins: When Intrinsic Higher Activity Is Flawed by Rapid Deactivation *Organometallics* **2019**, *38*, 2664-2673.
38. Ehm, C.; Vittoria, A.; Goryunov, J. P.; Izmer, V. V.; Kononovich, D. S.; Samsonov, O. V.; Budzelaar, P. H. M.; Voskoboynikov, A. Z.; Busico, V. Uborsky, D. V.; Cipullo, R. On the Limits of Tuning Comonomer Affinity of ‘Spaleck-type’ Ansa-Zirconocenes in Ethene/1-Hexene Copolymerization: a High-Throughput Experimentation/QSAR Approach. *Dalton Trans.* **2020**, *49*, 10162–10172.
39. Zhang, M.; Colby, R. H.; Milner, S. T.; Chung, T. C. M.; Huang, T.; de Groot, W. Synthesis and Characterization of Maleic Anhydride Grafted Polypropylene with a Well-Defined Molecular Structure. *Macromolecules* **2013**, *46*, 4313–4323.
40. Ginzburg, A.; Ramakrishnan, V.; Rongo, L.; Rozanski, A.; Bouyahyi, M.; Jasinska-Walc, L.; Duchateau, R. The Influence of Polypropylene-Block/Graft-Polycaprolactone Copolymers on Melt Rheology, Morphology, and Dielectric Properties of Polypropylene/Polycarbonate Blends. *Rheo. Act.* **2020**, *59*, 601–619.

41. Nyangoye, O, N.; Li, T.; Chen, L.; Cai, Z. Reactivity Comparison of ω -Alkenols and Higher 1-Alkenes in Copolymerization with Propylene using an Isospecific Zirconocene-MMAO Catalyst. *Polymers* **2015**, *7*, 2009–2016.
42. Hendriksen, C.; Friederichs, F.; Sainani, J. B.; Chatteree, A.; Izmer, V.; Kononovich, D.; Voskoboynikov, A.; Busico, V.; Cipullo, R.; Vittoria, A. WO 2020/043815 A1 to SABIC Global Technologies B.V.
43. Kaminsky, W. Polyolefins: 50 Years after Ziegler and Natta II-Polyolefins by Metallocenes and other Single-Site Catalysts. *Adv. Pol. Sci.* 258.
44. Chien J, C, W.; He, D. Olefin Copolymerization with Metallocene Catalysts. I. Comparison of Catalysts. *J. Polym. Sci. Polym. Chem.* **1991**, *29*, 1585–1593.
45. Heiland K.; Kaminsky, W. Comparison of Zirconocene and Hafnocene Catalysts for the Polymerization of Ethylene and 1-Butene *Makromol. Chem.* **1992**, *193*, 601–610.
46. Karssenberg, F, G.; Wang, B.; Friederichs, N.; Mathot, V, B, F. Terminal and Penultimate Reactivity Ratios in Single-Site Ethene/Propene Copolymerizations: Comparison of Kakugo and Direct Peak Methods *Macromol. Chem. Phys.* **2005**, *206*, 1675–1683.
47. For methods 1-2, see for example: Kissin, Y.; Brandolini, A.; Garlick, J. L. Kinetics of Ethylene Polymerization Reactions with Chromium Oxide Catalysts. *J. Pol. Sci.: Part A: Pol. Chem.* **46**, 5315–5329.
48. For method 3, see: Fineman, M.; Ross, S, D. Linear Method for Determining Monomer Reactivity Ratios in Copolymerization. *J. Polym. Sci.* **1950**, *5*, 259–265.
49. Aaltonen, P.; Fink, G.; Loefgren, B.; Seppaelae, J. Synthesis of Hydroxyl Group Containing Polyolefins with Metallocene/Methylaluminumoxane Catalysts *Macromolecules* **1996**, *29*, 5255–5260.

For Table of Contents use only

